Production of $\chi_{c1}(3872)$ and $T_{\psi\psi}(6900)$ from hadronic collisions to ultraperipheral collisions at EIC

Wolfgang Schäfer [1],

[1] Institute of Nuclear Physics, Polish Academy of Sciences, Kraków

Exotic heavy meson spectroscopy and structure with EIC, 15.-19. August 2022

Outline

Production of X(3872) in hadronic collisions - gluon gluon fusion

Ultraperipheral collisions, $\gamma\gamma$ collisions at EIC

What is the mechanism of $T_{\psi\psi}(6900)$ in pp collisions?

$T_{\psi\psi}(6900)$ in UPCs

A. Cisek, W. Schäfer and A. Szczurek, "Structure and production mechanism of the enigmatic $X(3872)$ in high-energy hadronic reactions," [arXiv:2203.07827 [hep-ph]].

R. Maciuła, W. Schäfer and A. Szczurek, "On the mechanism of $T_{4c}(6900)$ tetraquark production," Phys. Lett. B **812** (2021), 136010 [arXiv:2009.02100 [hep-ph]].

I. Babiarz, R. Pasechnik, W. Schäfer and A. Szczurek, "Light-front approach to axial-vector quarkonium $\gamma^*\gamma^*$ form factors," [arXiv:2208.05377 [hep-ph]].

S. Baranov, A. Cisek, M. Kłusek-Gawenda, W. Schäfer and A. Szczurek, "The $\gamma\gamma \to J/\psi J/\psi$ reaction and the $J/\psi J/\psi$ pair production in exclusive ultraperipheral ultrarelativistic heavy ion collisions," Eur. Phys. J. C **73** (2013) no.2, 2335 [arXiv:1208.5917 [hep-ph]].

Hadroproduction of $X(3872)$ (or $\chi_{c1}(3872)$)

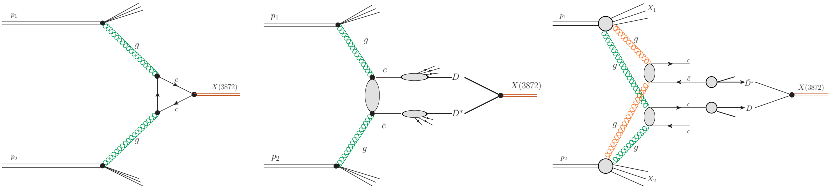

- Structure of $\chi_{c1}(3872)$ ($J^{PC} = 1^{++}$) still enigmatic. Its situation near the threshold of $D\bar{D}^*$ suggests its interpretation as the weakly bound “molecule”.
- What about a $\chi_{c1}(2P)$ component?
- Production at large p_T (hard process) is often suggested to serve as a probe of structure.
- P_T distributions have been measured by ATLAS, CMS and LHCb in the $J/\psi\pi\pi$ channel.
- Do the sizeable production cross sections rule out the large size molecule?
- We use the k_T-factorization approach in which gluons carry transverse momentum and are off-shell. It efficiently includes some NLO corrections at small-x. Note that for on-shell gluons $gg \to 1^{++}$ vanishes!

k_T-factorization: fusion of off-shell gluons: $c\bar{c}$ state

The inclusive cross section for $X(3872)$-production via the $2 \to 1$ gluon-gluon fusion mode is obtained from

$$\frac{d\sigma}{dy d^2\boldsymbol{p}} = \int \frac{d^2\boldsymbol{q}_1}{\pi \boldsymbol{q}_1^2} \mathcal{F}(x_1, \boldsymbol{q}_1^2, \mu_F^2) \int \frac{d^2\boldsymbol{q}_2}{\pi \boldsymbol{q}_2^2} \mathcal{F}(x_2, \boldsymbol{q}_2^2, \mu_F^2)\, \delta^{(2)}(\boldsymbol{q}_1 + \boldsymbol{q}_2 - \boldsymbol{p}) \times \frac{\pi}{(x_1 x_2 s)^2} \overline{|\mathcal{M}_{g^* g^* \to X(3872)}|^2} \,.$$

With

$$\mathcal{M}_{g^* g^* \to X(3872)} = \frac{q_{1\perp}^{\mu} q_{2\perp}^{\nu}}{|\boldsymbol{q}_1||\boldsymbol{q}_2|} \mathcal{M}_{\mu\nu} = \frac{x_1 x_2 s}{|\boldsymbol{q}_1||\boldsymbol{q}_2|} n_+^{\mu} n_-^{\nu} \mathcal{M}_{\mu\nu}$$

Here the matrix element squared for the fusion of two off-shell gluons into the $^3P_1$ color singlet $c\bar{c}$ charmonium is (Kniehl, Vasin, Saleev):

$$\overline{|n_+^{\mu} n_-^{\nu} \mathcal{M}_{\mu\nu}|^2} = \frac{(4\pi\alpha_S)^2}{N_c(N_c^2 - 1)} \frac{|R'(0)|^2}{\pi M_X^3} \frac{\boldsymbol{q}_1^2 \boldsymbol{q}_2^2}{(M_X^2 + \boldsymbol{q}_1^2 + \boldsymbol{q}_2^2)^4} \times \Big((\boldsymbol{q}_1^2 + \boldsymbol{q}_2^2)^2 \sin^2\phi + M_X^2 (\boldsymbol{q}_1^2 + \boldsymbol{q}_2^2 - 2|\boldsymbol{q}_1||\boldsymbol{q}_2| \cos\phi) \Big) \,,$$

where ϕ is the azimuthal angle between $\boldsymbol{q}_1, \boldsymbol{q}_2$. The momentum fractions of gluons are fixed as $x_{1,2} = m_T \exp(\pm y)/\sqrt{s}$, where $m_T^2 = \boldsymbol{p}^2 + M_X^2$. We use for the first radial p-wave excitation from $|R'(0)|^2 = 0.1767\,\mathrm{GeV}^5$ from Eichten & Quigg.

Production of molecule component

- Here we also start from the hard subprocess: production of the $c\bar{c}$-pair.

$$\frac{d\sigma(pp \to Q\bar{Q} + \mathrm{anything})}{dy_1 dy_2 d^2\boldsymbol{p}_1 d^2\boldsymbol{p}_2} = \int \frac{d^2\boldsymbol{k}_1}{\pi \boldsymbol{k}_1^2} \mathcal{F}(x_1, \boldsymbol{k}_1^2, \mu_F^2) \int \frac{d^2\boldsymbol{k}_2}{\pi \boldsymbol{k}_2^2} \mathcal{F}(x_2, \boldsymbol{k}_2^2, \mu_F^2)$$
$$\times \delta^{(2)}\left(\boldsymbol{k}_1 + \boldsymbol{k}_2 - \boldsymbol{p}_1 - \boldsymbol{p}_2\right) \frac{1}{16\pi^2 (x_1 x_2 s)^2} \overline{|\mathcal{M}^{\mathrm{off-shell}}_{g^* g^* \to c\bar{c}}|^2} .$$

where $\mathcal{M}^{\mathrm{off-shell}}_{g^* g^* \to Q\bar{Q}}$ is the off-shell matrix element for the hard subprocess (Catani, Ciafaloni, Hautmann).

- we then hadronize charm quarks to $D, \bar{D}^*$ mesons, by assuming, in the pp-cm frame, that

$$\vec{p}_D = \vec{p}_c .$$

- We use fragmentation fractions:

$$f(c \to D^0) = f(\bar{c} \to \bar{D}^0) = 0.547 ,$$
$$f(c \to D^+) = f(\bar{c} \to D^-) = 0.227 ,$$
$$f(c \to D^{*0}) = f(\bar{c} \to \bar{D}^{*0}) = 0.237 ,$$
$$f(c \to D^{*+}) = f(\bar{c} \to \bar{D}^{*-}) = 0.237 .$$

Production of molecule component

- The molecule is the C-even combination

$$|\Psi_{mol}\rangle = \frac{1}{\sqrt{2}}\left(|D^0\bar{D}^{*0}\rangle + |D^{*0}\bar{D}^0\rangle\right) \; .$$

- To obtain $D, \bar{D}^*$, we multiply the $c\bar{c}$ cross section by

$$\frac{1}{2}[f(c\to D^0)f(\bar{c}\to\bar{D}^{*0}) + f(c\to D^{*0})f(\bar{c}\to\bar{D}^0)] = \begin{cases} 0.036 \text{ direct} \\ 0.13 \text{ including feeddown.} \end{cases}$$

- In the spirit of effective range theory, we want to relate the continuum cross section to the bound state cross section.
- We are interested in low

$$k_{rel} = \frac{1}{2}\sqrt{M_{c\bar{c}}^2 - 4m_c^2}\;,$$

  We integrate the $D\bar{D}^*$ cross section over the relative momentum $k_{rel}^{D\bar{D}^*}$ up to a cutoff $k_{max}^{D\bar{D}}$ (Artoisenet & Braaten). Instead impose a cutoff k_{max} on the relative momentum k_{rel}. Within our kinematics the latter will be similar to $k_{rel}^{D\bar{D}^*}$, but somewhat larger. We estimate, that $k_{max} = 0.2\,\mathrm{GeV}$ corresponds roughly to $k_{max}^{DD} \approx 0.13\,\mathrm{GeV}$.

Production of molecule component

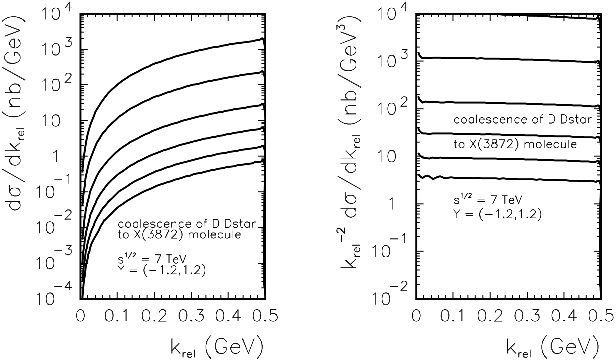

Figure: Distribution in k_{rel} for different windows of $p_{t,c\bar{c}} = p_{t,X}$ (left panel) for the CMS kinematics. In the right panel we show the cross sections divided by k_{rel}^2. In these calculations the KMR UGDF with the MMHT NLO collinear gluon distribution was used. Branching fractions are included here.

- cross section $d\sigma \propto k_{rel}^2 dk_{rel}$, cubic dependence on cutoff.
- debate in the literature on $k_{max}^{D\bar{D}^*}$, some authors suggest $k_X = \sqrt{2\mu\varepsilon_X} \sim 35\,\mathrm{MeV}$, but more consistent with effective range theory is $k_{max}^{D\bar{D}^*} \sim m_\pi$.
- better would be a calculation with a $D\bar{D}^*$ "wave function at the origin".

Numerical results vs. data, CMS

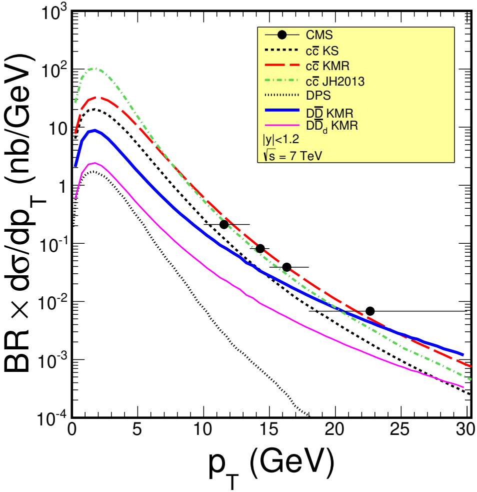

Figure: Transverse momentum distribution of $X(3872)$ for the CMS experiment. Shown are results for 3 different gluon uPDFs. Here BR $= 0.038$. The upper limit for the SPS molecular scenario is shown as the thick solid line. The thin solid line shows the molecular scenario neglecting the feeddown component of D^0, $\bar{D}^0$. We also show corresponding distribution for the DPS mechanism (dotted line).

Numerical results vs. data, ATLAS

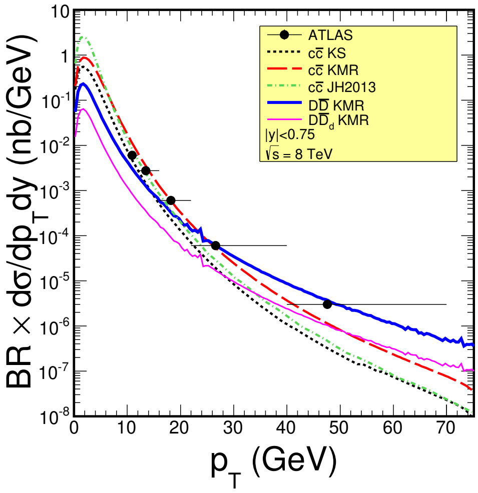

Figure: Transverse momentum distribution of $X(3872)$ for the ATLAS experiment. Shown are results for 3 different gluon uPDFs. Here $\mathrm{BR} = 0.038 \cdot 0.0596$. The upper limit for the SPS molecular scenario is shown as the thick solid line. The thin solid line shows the molecular scenario neglecting the feeddown component of $D^0, \bar{D}^0$.

Numerical results vs. data, LHCb

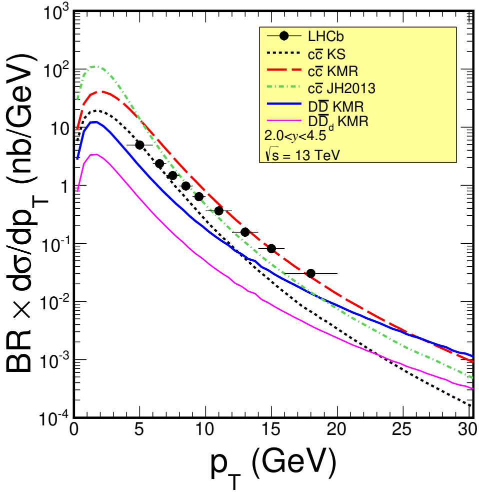

Figure: Transverse momentum distribution of $X(3872)$ for the LHCb experiment. Shown are results for 3 different gluon uPDFs. Here BR = 0.038. The upper limit for the SPS molecular scenario is shown as the thick solid line. The thin solid line shows the molecular scenario neglecting the feeddown component of $D^0, \bar{D}^0$.

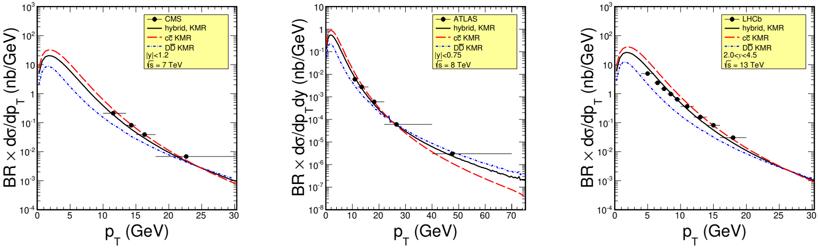

Figure: Transverse momentum distribution of $X(3872)$ for the CMS, ATLAS and LHCb experiments. Shown are results for the KMR UGDF. Here BR $= 0.038$ for CMS and LHCb, and $\mathrm{BR} = 0.038 \cdot 0.0596$ for ATLAS. We show results for different combinations of α and β as specified in the figure legend. Here the feedown contributions are included.

- $$|X(3782)\rangle = \alpha|c\bar{c}\rangle + \frac{\beta}{\sqrt{2}}\left(|D\bar{D}^*\rangle + |\bar{D}D^*\rangle\right) \ .$$

Ultraperipheral collisions

some examples of ultraperipheral processes:

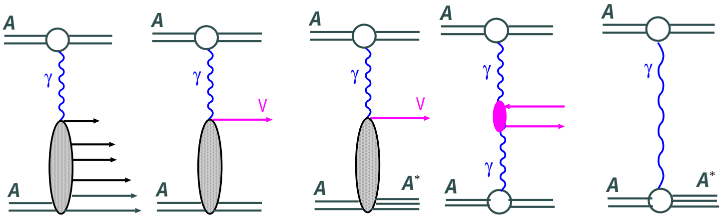

- photoabsorption on a nucleus
- diffractive photoproduction with and without breakup/excitation of a nucleus
- $\gamma\gamma$-fusion.
- electromagnetic excitation/dissociation of nuclei. Excitation of Giant Dipole Resonances.
- the intact nuclei in the final state are not measured. Each of the photon exchanges is associated with a large rapidity gap.
- very small p_T of the photoproduced system.

Ultraperipheral collisions

Photon-photon process in the electron-proton or electron-ion collision:

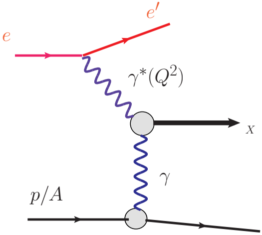

- proton ($Z = 1$) or ion ($Z = 82$ for Pb) is a source of quasireal Weizsäcker-Williams photons)

$$n(x) = \frac{Z^2\alpha_{\rm em}}{\pi} \int \frac{d\boldsymbol{q}^2}{\boldsymbol{q}^2} \left(\frac{\boldsymbol{q}^2}{\boldsymbol{q}^2 + x^2 m_p^2} \right)^2 F_{\rm ch}^2(\boldsymbol{q}^2 + x^2 m_p^2)$$

- "anti-tagged" electrons, say $Q^2 < 0.1\,\mathrm{GeV}^2$, are also the source of quasireal photons $\longrightarrow$ $\gamma\gamma$-fusion.
- at finite Q^2 we have access to a whole polarization density matrix of virtual photons,
- the intact nuclei in the final state are not measured. Photon exchange is associated with a large rapidity gap.

$\gamma^*\gamma^*$-transition form factors for $J^{PC} = 1^{++}$ axial mesons

$$
\begin{aligned}
\frac{1}{4\pi\alpha_{\rm em}}\mathcal{M}_{\mu\nu\rho} &= i\left(q_1 - q_2 + \frac{Q_1^2 - Q_2^2}{(q_1+q_2)^2}(q_1+q_2)\right)_\rho \tilde{G}_{\mu\nu}\,\frac{M}{2X}F_{\rm TT}(Q_1^2, Q_2^2) \\
&+ \quad i e^L_\mu(q_1)\tilde{G}_{\nu\rho}\,\frac{1}{\sqrt{X}}F_{\rm LT}(Q_1^2, Q_2^2) + i e^L_\nu(q_2)\tilde{G}_{\mu\rho}\,\frac{1}{\sqrt{X}}F_{\rm TL}(Q_1^2, Q_2^2)\,.
\end{aligned}
$$

- Above we introduced

$$
\tilde{G}_{\mu\nu} = \varepsilon_{\mu\nu\alpha\beta}\, q_1^\alpha q_2^\beta\,,
$$

  and the polarization vectors of longitudinal photons

$$
e^L_\mu(q_1) = \sqrt{\frac{-q_1^2}{X}}\left(q_{2\mu} - \frac{q_1\cdot q_2}{q_1^2}q_{1\mu}\right), \qquad e^L_\nu(q_2) = \sqrt{\frac{-q_2^2}{X}}\left(q_{1\nu} - \frac{q_1\cdot q_2}{q_2^2}q_{2\nu}\right).
$$

- $F_{\rm TT}(0,0) = 0$, there is no decay to two photons (Landau-Yang).
- $F_{\rm LT}(Q^2,0) \propto Q$ (absence of kinematical singularities). $f_{\rm LT} = \lim_{Q^2\to 0} F_{\rm LT}(Q^2,0)/Q$ gives rise to so-called "reduced width".
- we are interested in the situation with one virtual and one real photon.

$\gamma^*\gamma^*$ cross sections

$$\sigma_{ij} = \frac{32\pi(2J+1)}{N_i N_j} \frac{\hat{s}}{2M\sqrt{X}} \frac{M\Gamma}{(\hat{s}-M^2)^2 + M^2\Gamma^2} \Gamma^{ij}_{\gamma^*\gamma^*}(Q_1^2, Q_2^2, \hat{s}),$$

where $\{i,j\} \in \{\mathrm{T},\mathrm{L}\}$, and $N_\mathrm{T} = 2, N_\mathrm{L} = 1$ are the numbers of polarization states of photons. In terms of our helicity form factor, we obtain for the LT configuration, putting at the resonance pole $\hat{s} \to M^2$, and $J = 1$ for the axial-vector meson:

$$\Gamma^{\mathrm{LT}}_{\gamma^*\gamma^*}(Q_1^2, Q_2^2, M^2) = \frac{\pi\alpha_{\mathrm{em}}^2}{3M} F^2_{\mathrm{LT}}(Q_1^2, Q_2^2).$$

$$\tilde{\Gamma}(A) = \lim_{Q^2\to 0} \frac{M^2}{Q^2} \Gamma^{\mathrm{LT}}_{\gamma^*\gamma^*}(Q^2, 0, M^2) = \frac{\pi\alpha_{\mathrm{em}}^2 M}{3} f^2_{\mathrm{LT}}, \quad \text{with } f_{\mathrm{LT}} = \lim_{Q^2\to 0} \frac{F_{\mathrm{LT}}(Q^2,0)}{Q},$$

which provides a useful measure of size of the relevant e^+e^- cross section in the $\gamma\gamma$ mode. For a $c\bar{c}$ state:

$$f_{\mathrm{LT}} = -e_f^2 M^2 \frac{\sqrt{3N_c}}{8\pi} \int_0^\infty \frac{dk\, k^2 u(k)}{(k^2+m_Q^2)^2} \frac{1}{\sqrt{M_{Q\bar{Q}}}} \left\{ \frac{2}{\beta^2} - \frac{1-\beta^2}{\beta^3} \log\left(\frac{1+\beta}{1-\beta}\right) \right\},$$

with

$$\beta = \frac{k}{\sqrt{k^2+m_Q^2}}, \qquad M_{Q\bar{Q}} = 2\sqrt{k^2+m_Q^2}.$$

Nonrelativistic limit

- Simple explicit expressions in terms of derivative of WF at the origin can be found in the nonrelativistic limit (Schuler, Berends, van Gulik '98):

$$
\begin{aligned}
F_{\rm TT}(Q_1^2, Q_2^2) &= 2e_f^2 \sqrt{\frac{6N_c}{\pi M^3}} R'(0) \, \frac{Q_1^2 - Q_2^2}{\nu} \,, \\
F_{\rm LT}(Q_1^2, Q_2^2) &= -2e_f^2 \sqrt{\frac{6N_c}{\pi M}} R'(0) \frac{(\nu + Q_2^2) Q_1}{\nu^2} \,, \\
F_{\rm TL}(Q_1^2, Q_2^2) &= 2e_f^2 \sqrt{\frac{6N_c}{\pi M}} R'(0) \frac{(\nu + Q_1^2) Q_2}{\nu^2} \,,
\end{aligned}
$$

  with $\nu = (M^2 + Q_1^2 + Q_2^2)/2$.
- reduced width:

$$
\tilde{\Gamma}(A) = \frac{2\alpha_{\rm em}^2 e_f^4 N_c}{m_Q^4} \, |R'(0)|^2 \,,
$$

- relativistic corrections in a light front approach in I.Babiarz, R. Pasechnik, WS, A. Szczurek, hep-ph/ 2208.05377.
- for one virtual & one real photon one obtains

$$
F_{\rm TT}(Q^2, 0) = -\frac{Q}{M} F_{\rm LT}(Q^2, 0) \,.
$$

$\gamma^*\gamma^*$-transition form factors for $\chi_{c1}(1P)$ axial mesons

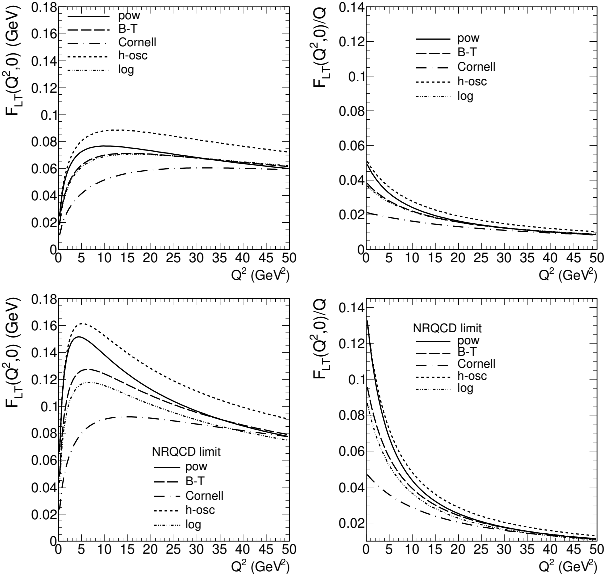

Figure: Form factors $F_{\rm LT}(Q^2,0)$ for one virtual photon (left and middle panels) and $F_{\rm LT}(Q^2,0)/Q$ (right panel). The top panels: our results in the LFWF approach and the bottom panels: nonrelativistic limit.

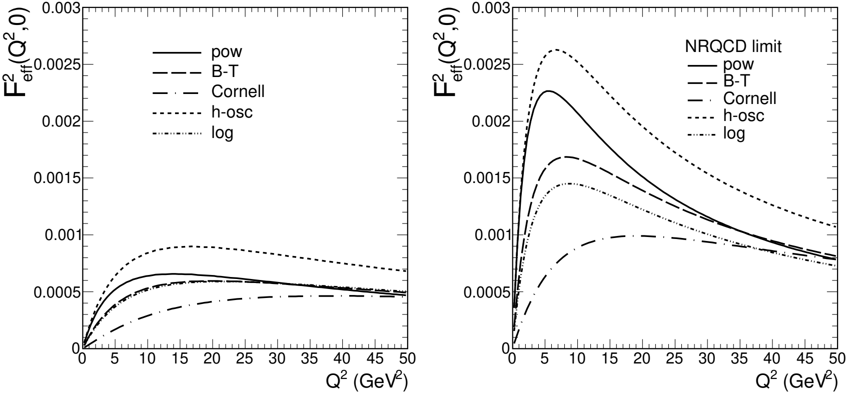

Figure: The square of the effective form factor as a function of photon virtuality within LFWF approach (on the l.h.s.) and in the nonrelativistic limit (on the r.h.s.).

$$\sigma^{\gamma^*\gamma}_{\rm tot}(Q^2,0) = 16\pi^3\alpha^2_{\rm em}\delta(\hat{s}-M^2)\,\frac{Q^2}{Q^2+M^2}\left(1+\frac{Q^2}{2M^2}\right)\left(\frac{F_{\rm LT}(Q^2,0)}{Q}\right)^2$$
$$\equiv 16\pi^3\alpha^2_{\rm em}\delta(\hat{s}-M^2)\,\mathrm{F}^2_{\rm eff}(Q^2)\,.$$

(Rough) Estimates for EIC energies

- for $Q^2 \ll 2M^2$ longitudinal photons will dominate. Note, that the total cross section does not have the dQ^2/Q^2 logarithmic integral.

$$Q^2 \frac{d\sigma(eA \to e' X(3872) A)}{dQ^2} = \frac{\alpha_{\rm em}}{\pi} \int_{y_{\rm min}}^{1} \frac{dy}{y} \frac{dx}{x} f_L(y) n_{\gamma/A}(x) \delta(xys - M^2) 16\pi^3 \alpha_{\rm em}^2 {\rm F}_{\rm eff}^2(Q^2)$$

- We assume the Q^2-dependence of a $c\bar{c}$-state, and a reduced width of $\tilde{\Gamma} = 0.5\,{\rm keV}$.
- limit on reduced width from Belle (updated, Achasov, 2022): $24\,{\rm eV} < \tilde{\Gamma}(\chi_{c1}(3872)) < 615\,{\rm eV}$.

Table: Cross sections on proton and ^{208}Pb

$\sqrt{s_{eN}}$ [GeV]	$\sigma(ep \to epX)$ [pb]	$\sigma(eA \to eAX)$ [pb]
50	0.06	60
140	0.16	340

- Hadronic contribution?

Possible molecule contribution to $\tilde{\Gamma}$?

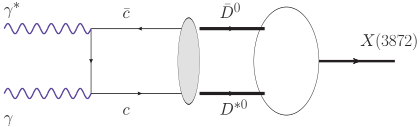

- apparently nothing (?) is known about the molecular contribution to the reduced width.
- What about the analogous contribution to the one we adopted in the hadronic case? Say $\gamma^*\gamma \to c\bar{c} \to \bar{D}D^*$, and FSI of $D\bar{D}^*$ generates the $X(3872)$.
- Spins of heavy quarks in $X(3872)$ are entangled to be in the spin-triplet state (M. Voloshin, 2004). But near threshold the $c\bar{c}$ state produced via $\gamma\gamma$-fusion is in the $^1S_0$ state. (It's different for gluons, where color octet populates $^3S_1$!)
- $\to$ "handbag mechanism" suppressed in heavy quark limit.
- Purely hadronic models?

Fully heavy tetraquark $T_{\psi\psi}(6900)$

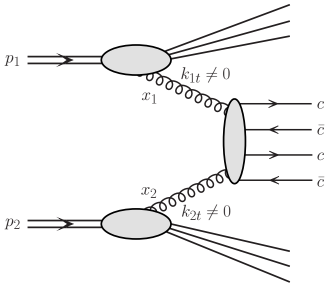

Figure: Two dominant reaction mechanisms of production of $c\bar{c}c\bar{c}$ nonresonant continuum. The left diagram represent the SPS mechanism (box type) and the left diagram the DPS mechanism.

$$d\sigma_{pp \to c\bar{c}c\bar{c}\,X} = \int dx_1 \frac{d^2 k_{1t}}{\pi k_{1t}^2} dx_2 \frac{d^2 k_{2t}}{\pi k_{2t}^2} \mathcal{F}_g(x_1, k_{1t}^2, \mu^2) \mathcal{F}_g(x_2, k_{2t}^2, \mu^2) d\hat{\sigma}_{g^* g^* \to c\bar{c}c\bar{c}} \,.$$

- Calculations performed using the code `KaTie` by A. van Hameren.

$T_{4c}(6900)$ single vs. double parton scattering

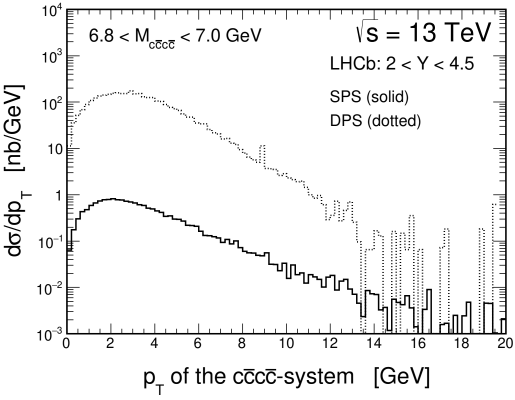

Figure: Distribution of $p_{t,4c}$ of four quark-antiquark system within invariant mass window $(M_R - 0.1\mathrm{GeV}, \mathrm{M_R} + 0.1\mathrm{GeV})$. Here $\sqrt{s} = 13$ TeV and average rapidity of quarks and antiquarks in the interval (2,4.5). The solid line is for SPS, the dashed line for $gggg \to c\bar{c}c\bar{c}$ DPS contribution.

$$\frac{d\sigma_{T_{4c}}}{d^3\vec{P}_{T_{4c}}} = F_{T_{4c}} \int_{M_{T_{4c}}-\Delta M}^{M_{T_{4c}}+\Delta M} d^3\vec{P}_{4c}\; dM_{4c} \frac{d\sigma_{c\bar{c}c\bar{c}}}{dM_{4c} d^3\vec{P}_{4c}} \delta^3(\vec{P}_{T_{4c}} - \frac{M_{T_{4c}}}{M_{4c}} \vec{P}_{4c})$$

Gluon-gluon fusion "color singlet model"

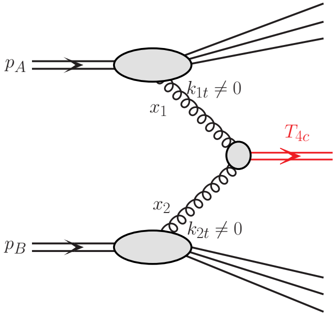

Figure: The mechanism of gluon-gluon fusion leading to the production of the $T_{4c}(6900)$ tetraquark.

The off-shell gluon fusion cross sections is proportional to a form-factor, which depends on the virtualities of gluons, $Q_i^2 = -k_i^2$:

$$d\sigma_{g^*g^*\to 0^-} \propto \frac{1}{k_{1t}^2 k_{2t}^2} (\vec{k}_{1t} \times \vec{k}_{2t})^2 F^2(Q_1^2, Q_2^2)\,,$$

$$d\sigma_{g^*g^*\to 0^+} \propto \frac{1}{k_{1t}^2 k_{2t}^2} \left((\vec{k}_{1t} \cdot \vec{k}_{2t})(M^2 + Q_1^2 + Q_2^2) + 2Q_1^2 Q_2^2 \right)^2 \frac{F^2(Q_1^2, Q_2^2)}{4X^2}\,,$$

with $X = (M^4 + 2(Q_1^2 + Q_2^2)M^2 + (Q_1^2 - Q_2^2)^2)/4$.

Production of pseudoscalar or scalar

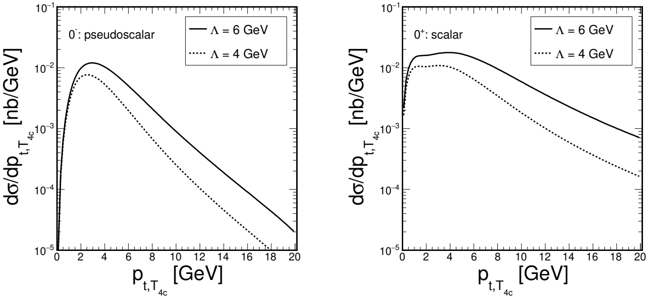

Figure: Transverse momentum distribution of the $T_{4c}(6900)$ tetraquark for the 0^- (left panel) and 0^+ (right panel) assignments. Here $\sqrt{s} = 13$ TeV. We show results for the KMR UGDF and $\Lambda = 6$ GeV (solid line) and $\Lambda = 4$ GeV (dashed line).

$$F(Q_1^2, Q_2^2) = \frac{\Lambda^2}{\Lambda^2 + Q_1^2 + Q_2^2} \ ,$$

- Since the ratio of signal-to-background improves with transverse momentum of the tetraquark and knowing relatively well the behaviour of the SPS and DPS background we can conclude that the 0^- assignment is disfavoured by the LHCb experimental results.

Possibilities of photoproduction of $T_{4c}(6900)$ in UPCs

- Production of $J/\psi J/\psi$ pairs in $\gamma\gamma$ collisions.

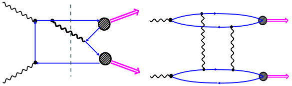

- Cross section in UPCs (lead-lead) at LHC (Baranov, Cisek, Kłusek-Gawenda, WS, Szczurek (2013)):

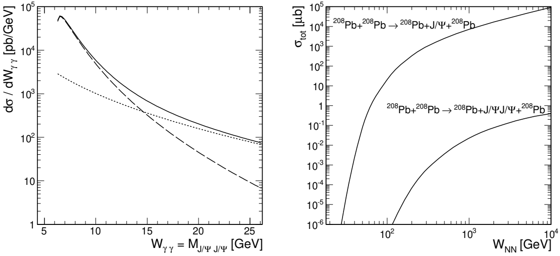

- Predictions for $T_{\psi\psi}$ in UPCs from the literature:
Goncalves & Moreira (2021): $\sigma_{tot} = 170\,\mathrm{nb}(0^+), 206(2^+)\,\mathrm{nb}$, incl. branching to $J/\psi J/\psi$.
Esposito et al. (2021): $\sigma_{tot} = (282\,\mathrm{or}\,1165) \times BR(J/\psi J/\psi)$ nb for $J^P = 0^+, 2^+$.

Possibilities of photoproduction of $T_{4c}(6900)$ in UPCs

- Here the cross section is dominated by transverse photons.
- Q^2 dependence and correlation of electron/hadronic plane could be used to investigate different spin-parity assignments.
- We estimate photoproduction cross section with $Q^2_{\rm max} = 0.1 \rm GeV$.
- No consensus on even the ballpark of the $\gamma\gamma$ width of $T_{4c}(6900)$ in the literature.
- We use $\Gamma = 2\,\rm keV$

Table: Cross sections on proton and ^{208}Pb

$\sqrt{s_{eN}}$ [GeV]	$\sigma(ep \to epT_{4c})$ [pb]	$\sigma(eA \to eAT_{4c})$ [pb]
50	0.06	21.3
140	0.256	360

Summary

- We considered prompt hadroproduction of $\chi_{c1}(3872)$ at LHC energies for a $c\bar{c}$ state, a molecule, or a mixture of both.
- The molecule production has the hardest behaviour as a function of p_T. This is expected from to the color-octet contribution. Shape of molecule alone does not agree well with data.
- Production of $c\bar{c}$ state gives reasonable behaviour, as does a mixture of $c\bar{c}$ and molecule.
- Electroproduction of $\chi_{c1}(3872)$ in the Coulomb field of a heavy nucleus may give access to form factor $F_{\rm LT}(Q^2, 0)$. This is additional information on the structure. We know how to calculate it for $c\bar{c}$, or possibly tetraquark states.
- What about the molecule? Can one calculate its reduced width to $\gamma_L^* \gamma$?
- Beyond exotics: these quantities haven't been measured even for $\chi_{c1}(1P)$.
- Production of fully heavy tetraquark potentially has large double parton scattering contribution.
- These complications make a clean environment such as $\gamma\gamma$ fusion in UPC very desirable.